Contents of this file

5 **Introduction**

The supplement consists of 6 text files, 10 figures and 3 tables. The individual sections contain an overview of the different modeling scenarios (Table S1), the precipitation time series created for testing the influence of the sequence of events (Fig. S1) and the table containing all distributions metrics for those 15 scenarios (Table S3), the tracer mass in storage, the cumulative tracer mass of the outflux and the cumulative mass balance errors for the 36 scenarios (Fig. S2), methods for the

10 computation of TTD metrics (Text S1, Fig. S3), methods for and results from the determination of young water fractions (Text S2, Fig. S4, Table S2), TTD smoothing (Text S3, Fig. S5), the derivation of TTDs from tracer breakthrough curves (Fig. S6), the analysis of spatial tracer distribution over the catchment and in its profile (Text S4, Fig. S7), outflow probability distributions plotted against cumulative outflow (Fig. S8), a method to add power law tails to AD or Gamma probability distributions (Text S5, Fig. S9) as well as an example of using TTDs for reactive solute transport applications

15 (Text S6, Fig. S10).

Text S1.

1) The first quartile (Q_1) was determined via the cumulative TTD. It is the transit time when 25 % of the applied tracer mass has left the system.

2) The median (Q_2) was derived similarly (when 50 % of the applied tracer mass has left the system).

3) The mean transit time (mTT) was calculated according to Eq. S1:

$$mTT = \sum (J_{out}^{norm} * \Delta t * t). \tag{S1}$$

4) The third quartile (Q_3) was again determined with the help of the cumulative TTD (when 75 % of the applied tracer mass has left the system).

5) The standard deviation (σ) is a measure describing the dispersion of a distribution, with a small standard deviation pointing towards the data point cloud being clustered closely around the mean. It was calculated according to Eq. S2:

$$\sigma = \sqrt{\sum (J_{out}^{norm} * \Delta t * t^2) - mTT^2} \,. \tag{S2}$$

6) The skewness (ν) is a measure that informs about how much a distribution leans to one side of its mean. A negative skew means that the distribution leans towards the right (the highest concentration follows after the mean), a positive skew indicates that the distribution leans towards the left (the highest concentration is reached before the mean). It was calculated according to Eq. S3:

$$\nu = \frac{\sum (J_{out}^{norm} * \Delta t * t^3) - (3 * mTT * \sigma^2) - mTT^3}{\sigma^3}. \tag{S3}$$

7) The excess kurtosis (γ) was calculated according to Eq. S4:

$$\gamma = \frac{\sum (J_{out}^{norm} * \Delta t * (t - mTT)^4)}{\sigma^4} - 3. \tag{S4}$$

A positive excess kurtosis means that a distribution produces more extreme outliers than the Gaussian normal distribution, so this measure is related predominantly to the tail of the distribution – and only to a lesser extent to its peak. For positive values of the excess kurtosis, the tail of the distribution approaches zero more slowly than a normal distribution while the peak is higher (leptokurtic). For negative values of the excess kurtosis, the tail approaches zero faster than a normal distribution while the peak is lower (platykurtic). There is no unanimous consent on the mathematical definition of what constitutes a "heavy" or "light" tail. According to some sources heavy tails are those tails that have more weight than an exponential tail – a definition which corresponds to heavy-tailed distributions being defined as possessing an increasing hazard (rate) function (Kellison and London, 2011). This definition would place Gamma distributions with shape parameters $\alpha < 1$ clearly in the category of heavy-tailed distributions and Gamma distributions with shape parameters $\alpha > 1$ in the category of light-tailed distributions. Other sources, however, attribute heavy tails only to distributions with infinite moment generating functions (Rolski et al, 2009). Therefore we are not using the (absolute) terms heavy-tailed or light-tailed to describe the TTDs but rather just refer to "heavier" and "lighter" tails.

Text S2.

We calculated young water fractions for the best-fit Gamma distributions to see how they are influenced by catchment and event properties. The young water fraction (F_{yw}) constitutes the fraction of water in discharge with an age below 2.3 months (Jasechko et al., 2016; Kirchner, 2016).

50   Modeled F_{yw} from the best-fit Gamma distributions ranged from 4 % to 100 % (Table S2). We also determined F_{yw} directly from the modeled TTDs. They ranged from 0 % to 61 %. The F_{yw} derived from the best-fit Gamma distributions and directly from the modeled TTDs differed considerably, especially for the scenarios with larger F_{yw}. The F_{yw} derived directly from the modeled TTDs were almost always smaller than the ones derived from the best-fit Gamma distributions.

In general, F_{yw} increases with increasing P_{sub}, θ_{ant}, K_S and with decreasing D_{soil} (Fig. S3). The highest F_{yw} was observed for

55   scenarios with shallow D_{soil}, wet θ_{ant} and large P_{sub}. Young water fractions increase with increasing θ_{ant}, because on the one hand, catchment soil storage is already filled and hydraulic conductivity of the soil is already high (close to saturation) so that the incoming event water can immediately flow laterally towards the outlet while only a smaller fraction stays in the soil storage or enters the low-conductivity bedrock. In catchments with higher K_S, F_{yw} also increases since the conductivity contrast between the bedrock and the soil increases and more of the incoming event water flows laterally towards the outlet

60   with a higher velocity. Shallow soils increase F_{yw} too due to the fact that less soil storage is available where event water can be stored before lateral flow is initiated. Finally, larger P_{sub} increases F_{yw} as well, which can be associated with the "flushing effect" where more flow in the more fully saturated soil layer equals a larger flux through the soil layer and hence a larger fraction of young water in the discharge.

Text S3.

65   The modeled TTDs where smoothed just for the purpose of better visual comparison – all the calculations and the fitting were performed on the unsmoothed data (see Fig. S4 for an example of a smoothed TTD). We smoothed the TTDs by using moving window averaging with increasing window size towards longer transit times according to Eq. S5 and S6:

$$N_{left}(t) = \begin{cases} N, & if \;\; (\ln t)^3 \leq 0 \\ \lfloor N(t) - 0.5(\ln t)^3 \rfloor, & if \;\; (\ln t)^3 > 0 \end{cases} \tag{S5}$$

$$N_{right}(t) = \begin{cases} N, & if \;\; (\ln t)^3 \leq 0 \\ \lfloor N(t) + (\ln t)^3 \rfloor, & if \;\; (\ln t)^3 > 0 \end{cases} \tag{S6}$$

70   with N_{left} being the model time step number at the left corner of the window, N_{right} the model time step number at the right corner of the window and N the model time step number at a given transit time t. We increased the window size with increasing transit time since we plotted the TTDs on a double-log scale so that the older parts of the TTDs were compressed and also because the variation in the initial shape of the TTD is higher and influenced less by the series of subsequent precipitation events.

75   **Text S4.**

Comparing the evolution of tracer concentrations throughout the model domain can explain the differences of the resulting TTDs for the various model scenarios. Figure S6 demonstrates this by showing tracer concentrations at the soil surface and

in a depth profile close to the center of the catchment for two very different scenarios (FHWB with the shortest median and mean transit time and TLDS with the longest median and mean transit time). The fast arrival of the tracer in the FHWB scenario is possible since the tracer quickly infiltrates the entire soil column and is transported laterally towards the outlet. In the TLDS scenario it takes much longer for the entire soil column to act as a pathway for lateral flow which is partly due to the fact that θ_{ant} is low (more pore space can be filled up until saturated hydraulic conductivity is reached and more pore space is available to be filled up before water will be diverted downslope at the bedrock–soil interface). Both TTDs peak after the entire soil column is filled with tracer and starts acting as a lateral flow path and some tracer has entered the bedrock. This happens almost instantly in the FHWB scenario and only after approximately 100 days in the TLDS scenario. The amount of tracer infiltrating into the bedrock is higher for the TLDS scenario. This is due to the fact that the contact time between tracer in the soil and the bedrock surface is longer. In the FHWB scenario the tracer is flushed out of the soil a lot faster (higher K_S and more P_{sub}), therefore less tracer can infiltrate into the bedrock. The soil in the FHWB scenario is virtually free of tracer much sooner than the soil in the TLDS scenario, therefore the power law tail of the TTD (deriving from the bedrock tracer outflux) starts earlier than for the TLDS scenario (around 1000 days vs. around 5000 days). The power law tails are heavier for TLDS since more tracer had the chance to infiltrate into the bedrock at late times.

Text S5.

Adding power law tails to Gamma or AD distributions can be done via a simple approach that replaces the tail of the respective distribution with a power law tail as soon as the probability density of the model distribution falls below that one of a power law with a constant a of 0.2 and an exponent k of 1.6 (Eq. S7 and Fig. S8):

$$f(t) = \begin{cases} t^{\alpha-1} \frac{e^{-\frac{t}{\beta}}}{\beta^{\alpha}\Gamma(\alpha)}, & if \quad t^{\alpha-1} \frac{e^{-\frac{t}{\beta}}}{\beta^{\alpha}\Gamma(\alpha)} \geq at^{-k} \ \lor \ t \leq \alpha\beta \\ at^{-k}, & if \quad t^{\alpha-1} \frac{e^{-\frac{t}{\beta}}}{\beta^{\alpha}\Gamma(\alpha)} < at^{-k} \ \land \ t > \alpha\beta \end{cases}. \tag{S7}$$

In order to preserve the mass balance, the combined distribution has to be re-normalized (accounting for the added mass from the power law tail, Eq. S8 and S9):

$$w = \int_{t=0}^{\infty} f(t). \tag{S8}$$

$$TTD(t) = \frac{f(t)}{w}. \tag{S9}$$

From a mass balance perspective, however, generally it is not necessary to add these power law tails since they only account for a very small fraction of the total injected mass. Yet they can alter the mTT significantly (while the median remains largely unaffected).

Text S6.

Modification of TTDs to incorporate reactive solute transport into the concept can be achieved, e.g., by multiplication of the TTD with a decay function. In this example an exponential decay function is used (Eq. S10):

$$TTD_{react}(t) = TTD(t) * e^{-t/t_{1/2}},\qquad\qquad\qquad\qquad\qquad\qquad\qquad\text{(S10)}$$

where TTD(t) is the probability density at transit time t and $t_{1/2}$ is the half-life of the solute. Note that the cumulative TTD_{react} does not add up to a value of 1 anymore. It rather reflects the fraction of solute that will eventually be discharged out of the catchment (Fig. S9).

Other functions that can modify TTDs to make them suitable predictors of reactive solute transport include specific retardation or removal functions for certain transit time ranges associated with flow paths through different catchment compartments (e.g., groundwater flow, soil matrix flow, macropore flow).
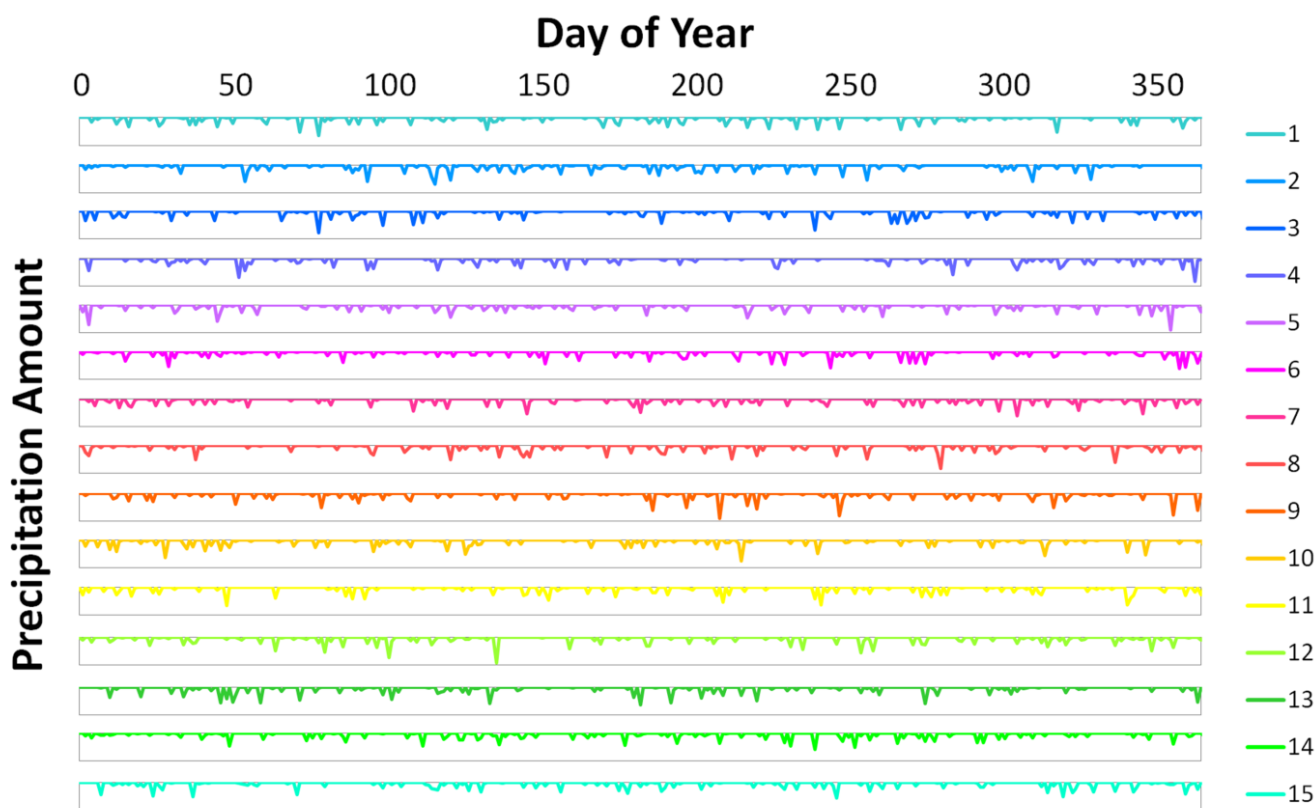
Figure S1: 15 different precipitation time series with similar exponential distributions of precipitation event amounts and interarrival times. The y-axes all range from 0 to 40 mm. The time series were created to test the influence of event sequence on the shape of TTDs.

120
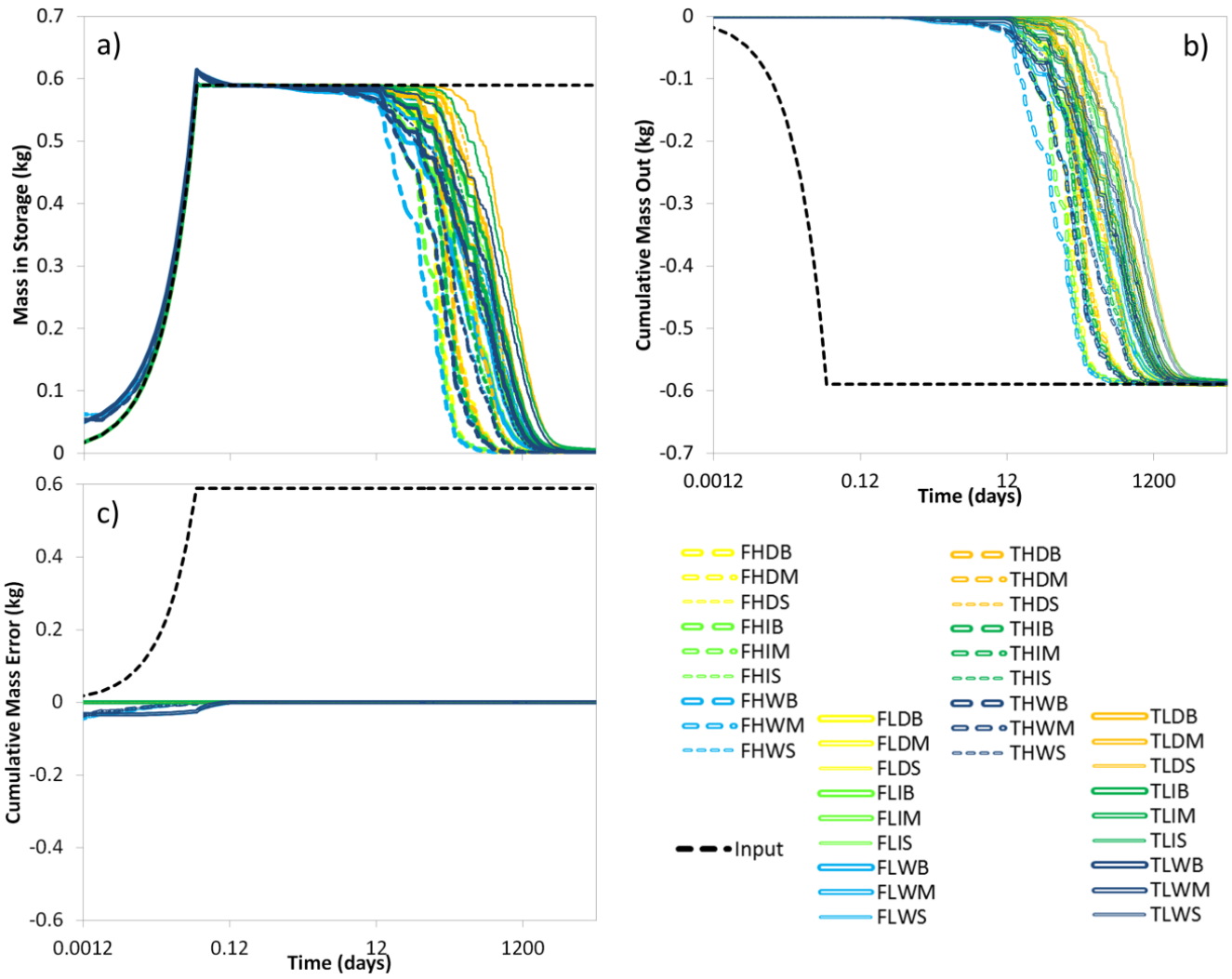
Figure S2: a) Total tracer mass in storage, b) cumulative tracer mass outflux, c) cumulative mass balance error for all 36 scenarios. Note that most scenarios plot on top of each other in panel c).
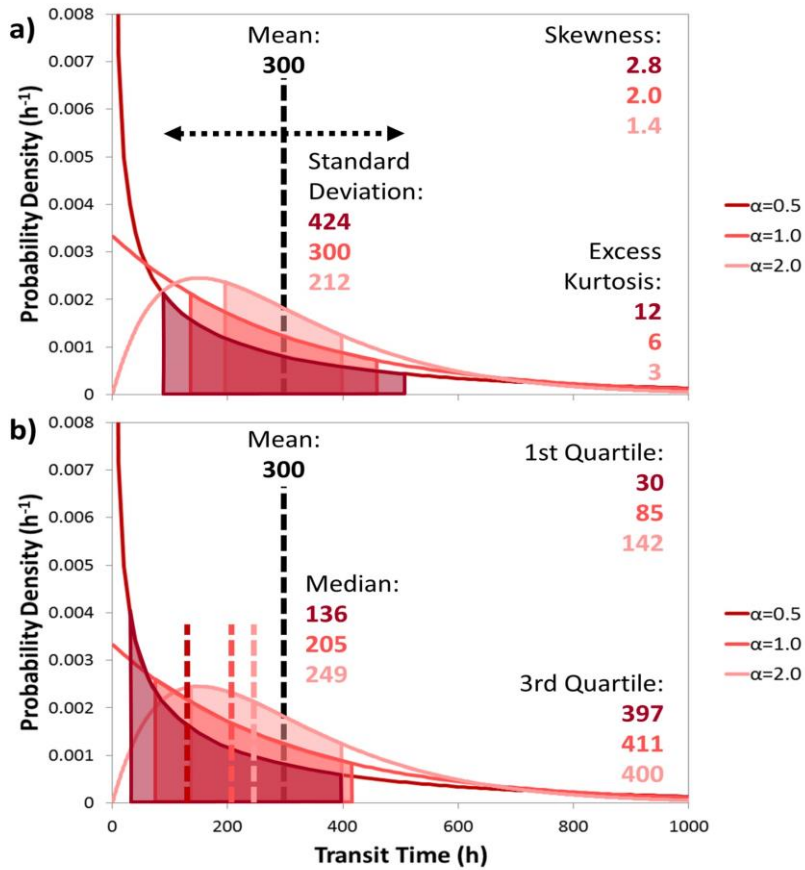
125 **Figure S3: Distribution metrics of three different Gamma distributions with varying shape parameter α and equal mean (300 h). a) Black dashed line: mean (300 h), dotted black line and filled areas under the curves: standard deviation. b) Black dashed line: mean (300 h), colored dashed lines: medians, filled areas under the curves range from the first to the third quartile (Q_1–Q_3).**
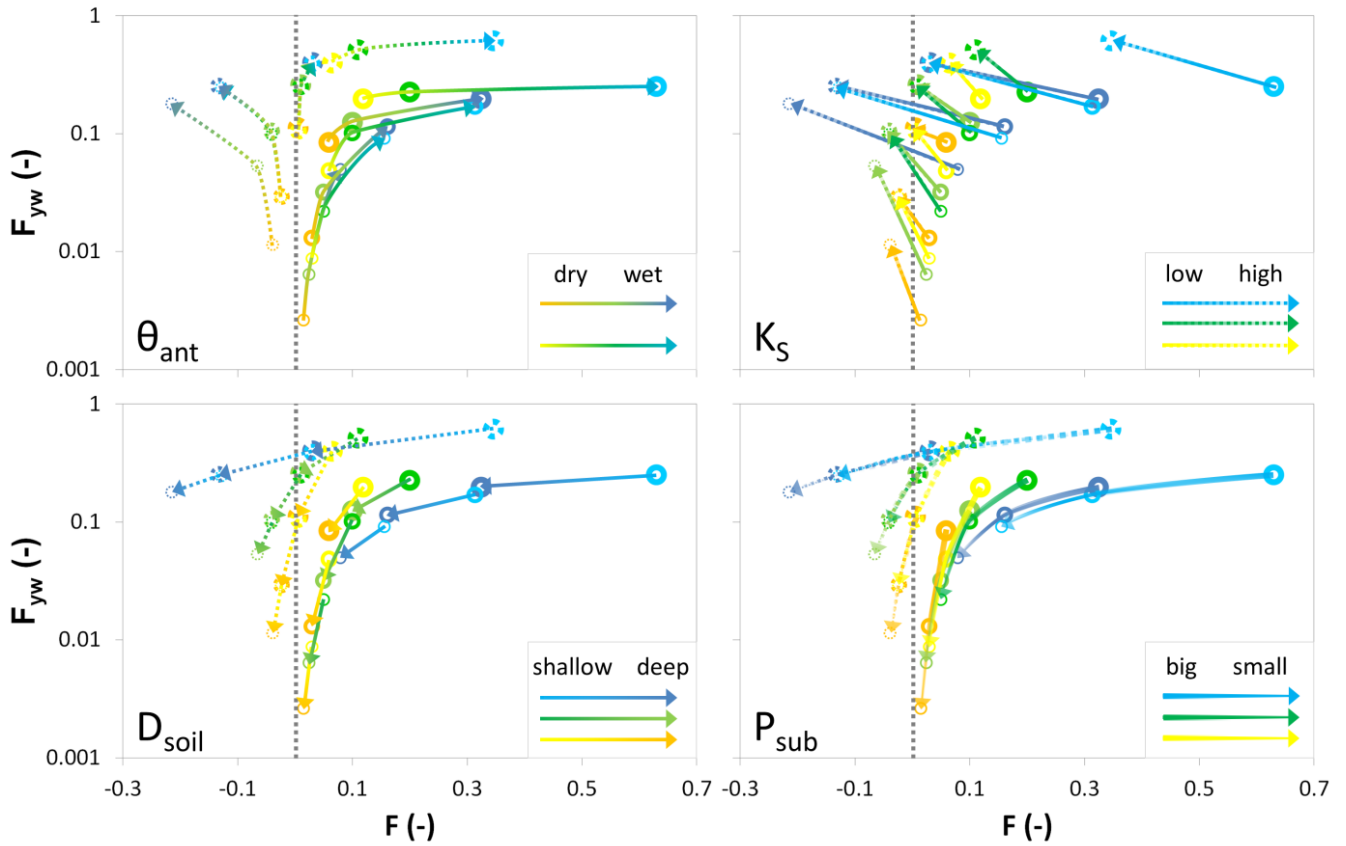
130   **Figure S4: Change of young water fractions (F_{yw}) with the flow path number (F) for four different catchment and climate properties. Yellow colors indicate dry, green intermediate and blue wet antecedent moisture conditions θ_{ant}. Thick marker lines indicate large, mid-sized lines medium and thin lines small amounts of subsequent precipitation P_{sub}. Solid lines indicate low, dashed lines high saturated hydraulic conductivities K_S, lighter shades of a color indicate shallow, darker shades deep soils D_{soil}.**
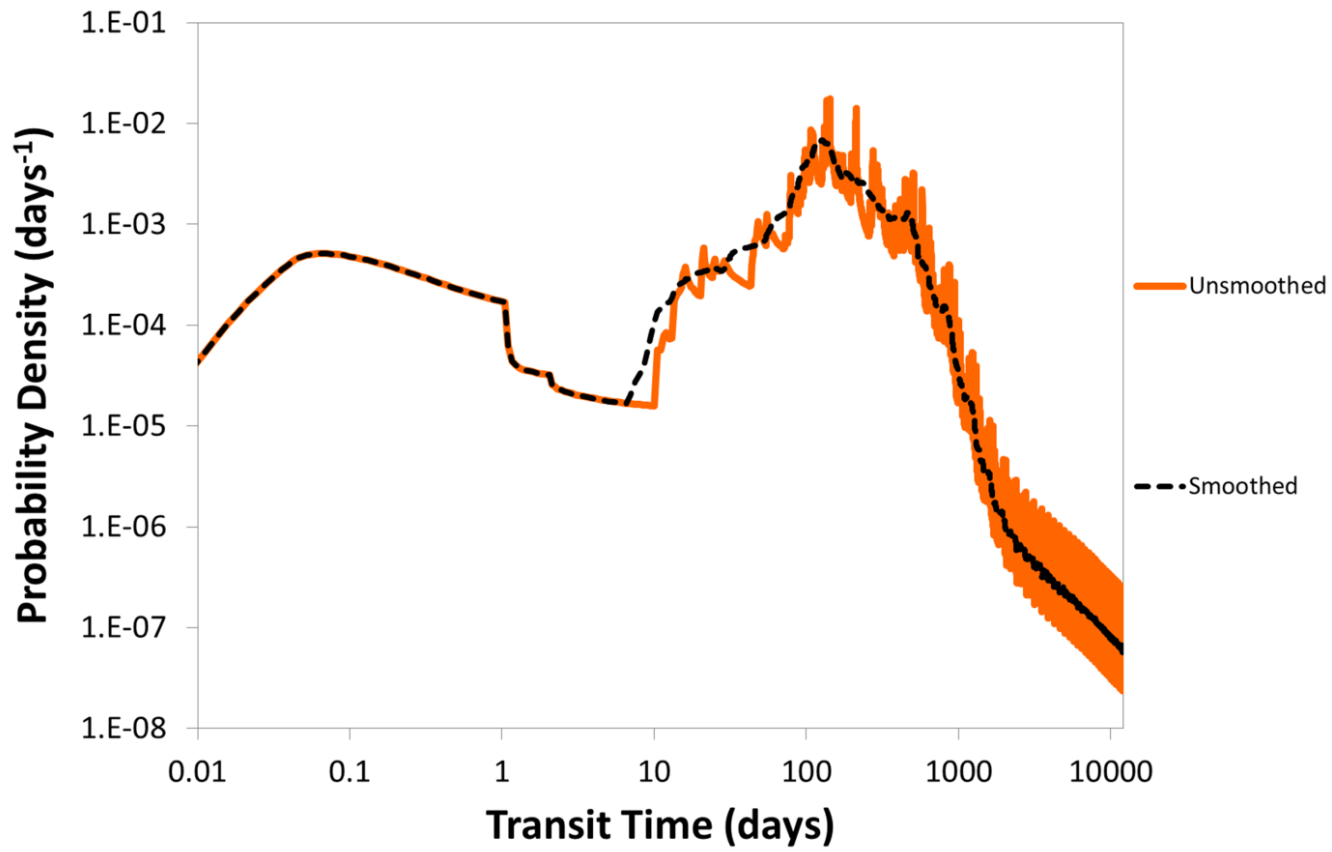
135

Figure S5: Unsmoothed (orange) and smoothed (black) version of one TTD.
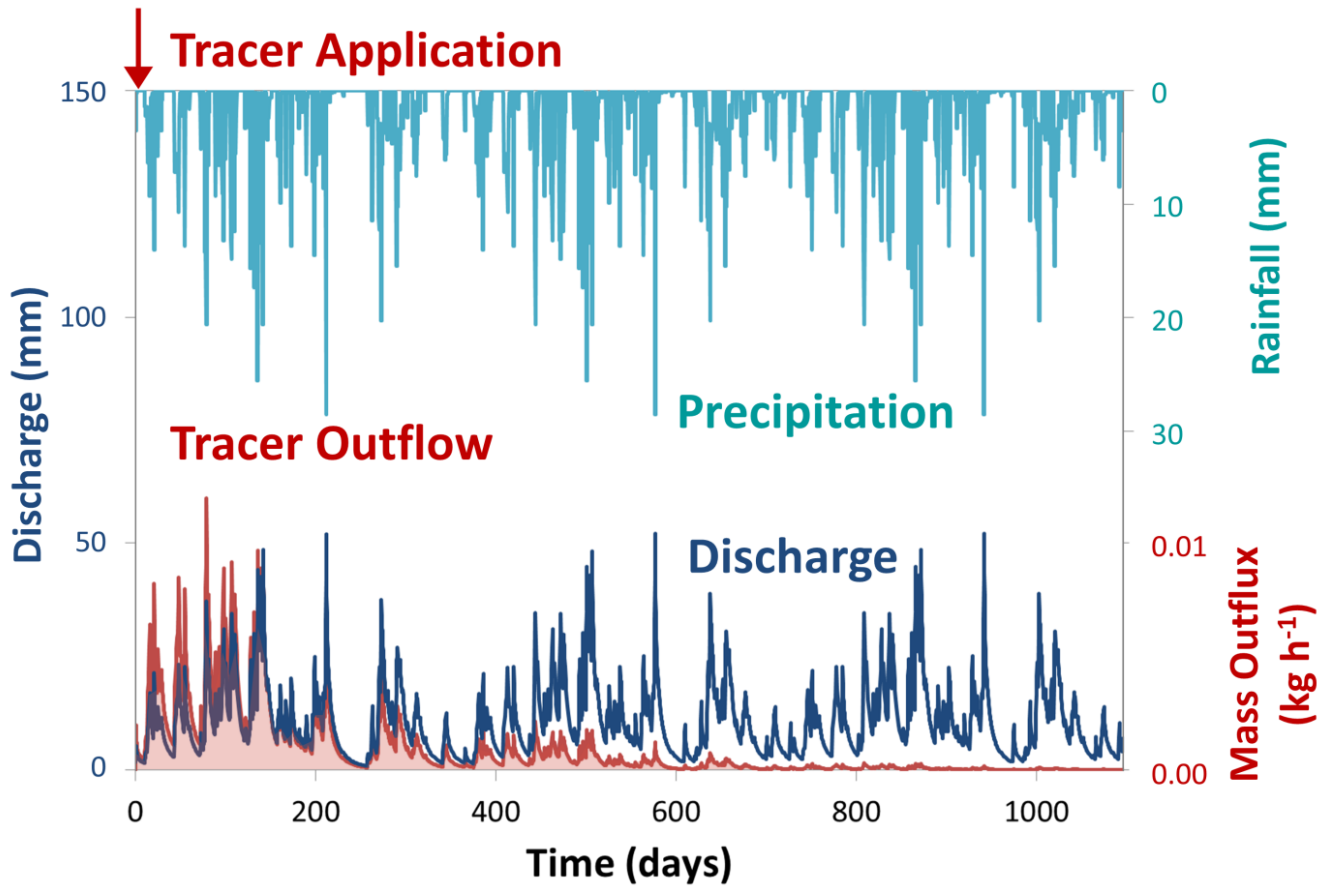
Figure S6: Precipitation input (cyan), total outflow (blue) and tracer concentration in the outflow (red) for the first three years of the model run for scenario THDM. The tracer breakthrough curve (when normalized) constitutes the TTD of the injected tracer impulse.

140
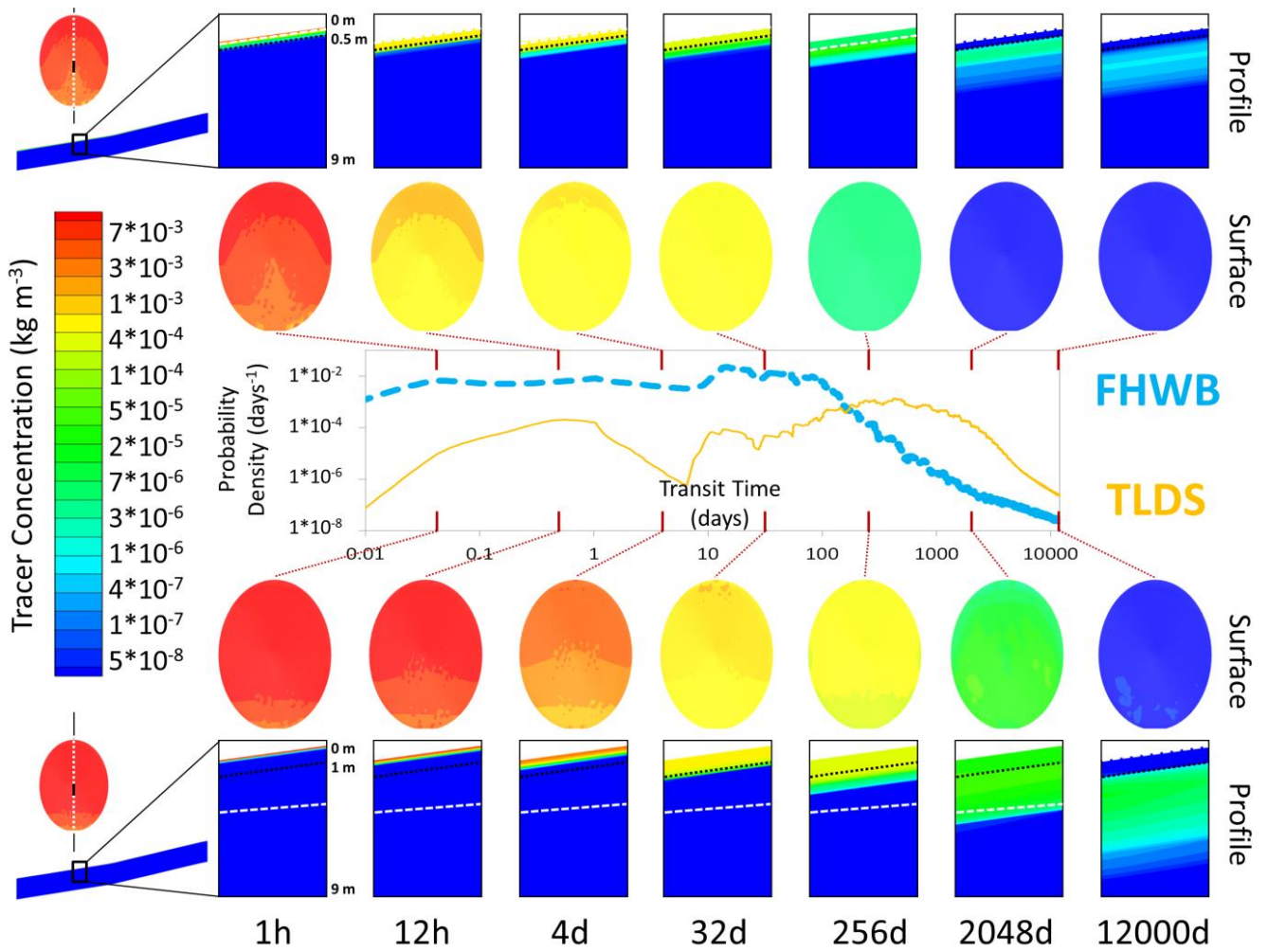
Figure S7: Time series of tracer concentration distribution in the surface soil across the entire catchment, in a depth profile in the center of the catchment for two scenarios (top: FHWB; bottom: TLDS) with very different resulting TTDs shapes. The dotted black line in the profiles represents the soil–bedrock interface; the white dashed line is the water table.
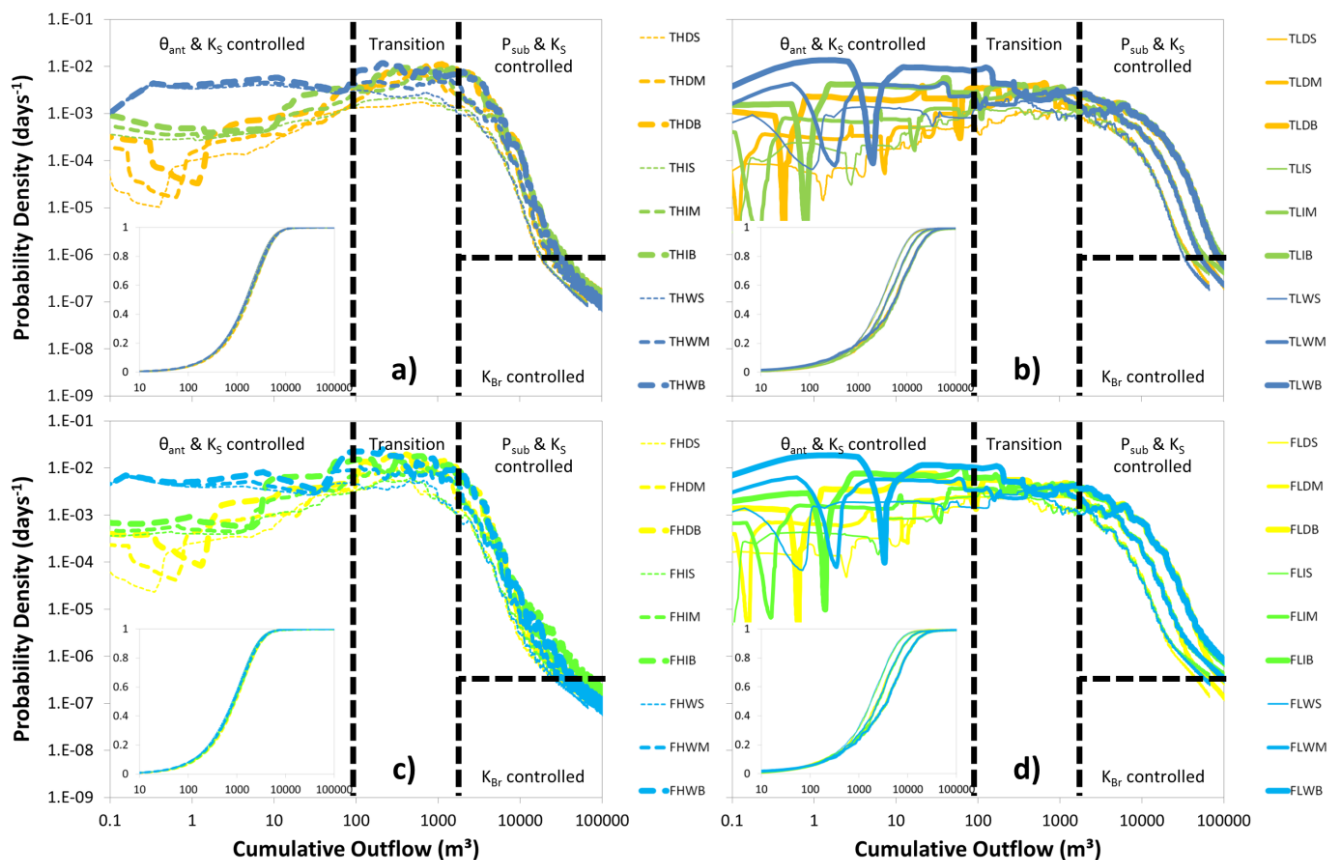
Figure S8: Similar to Fig. 7 except for the fact that outflow probability is plotted against cumulative outflow instead of transit time. Distributions are grouped by soil depth (upper panels a and b = deep (thick); lower panels c and d = shallow (flat)) and saturated hydraulic conductivity (left panels a and c = high; right panels b and d = low). Yellow colors indicate dry, green intermediate and blue wet antecedent moisture conditions. Thick lines indicate large, mid-sized lines medium and thin lines small amounts of subsequent precipitation amounts. Insets show cumulative outflow probability distributions. Dashed black lines divide TTDs into four parts, each part controlled by different properties. Note the log-log axes.
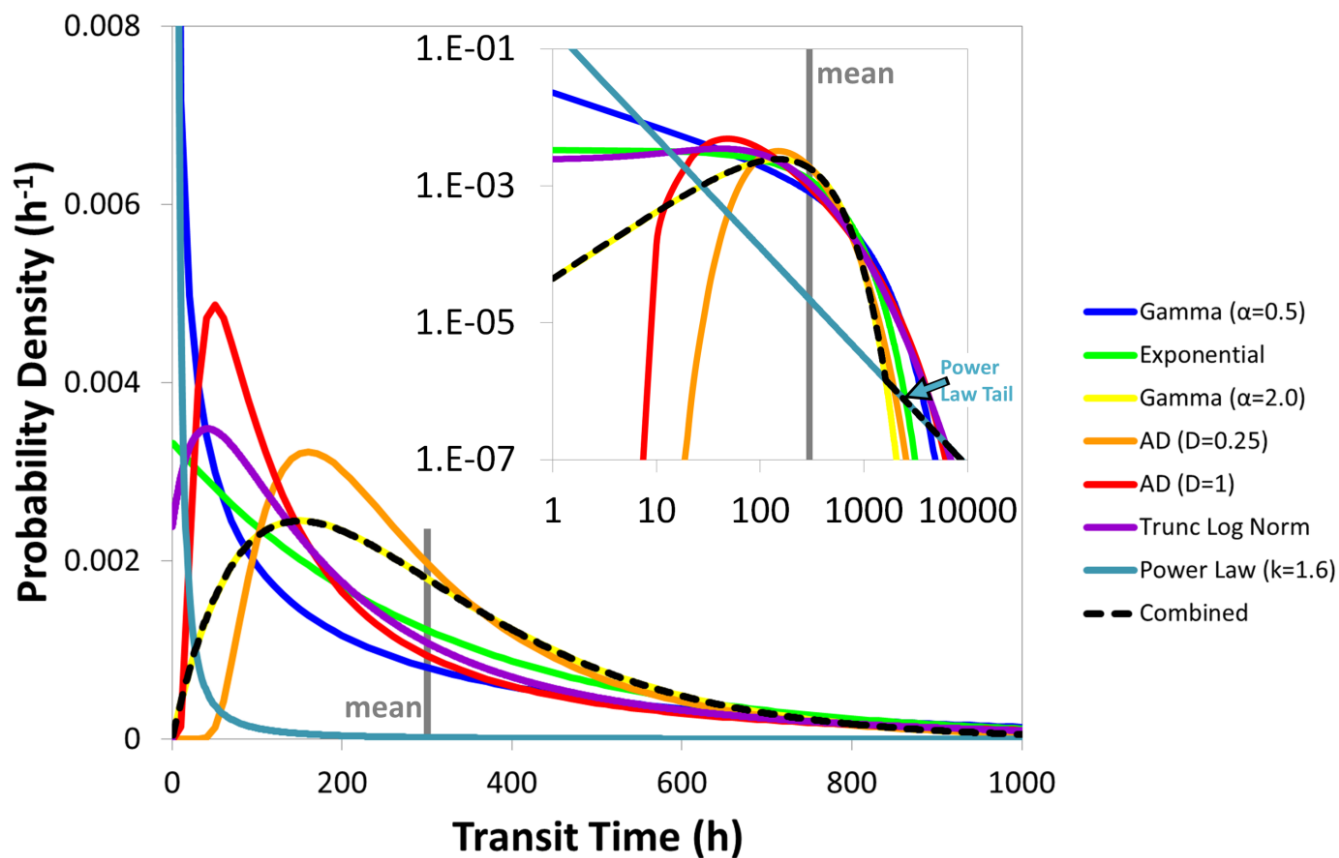
Figure S9: A set of seven different common theoretical probability distributions (all but the power law having a mean value of 300 h, grey line). The black dashed line is a distribution that is a combination of a Gamma distribution with the tail of a power law distribution. The inset has a log-log scale.

160
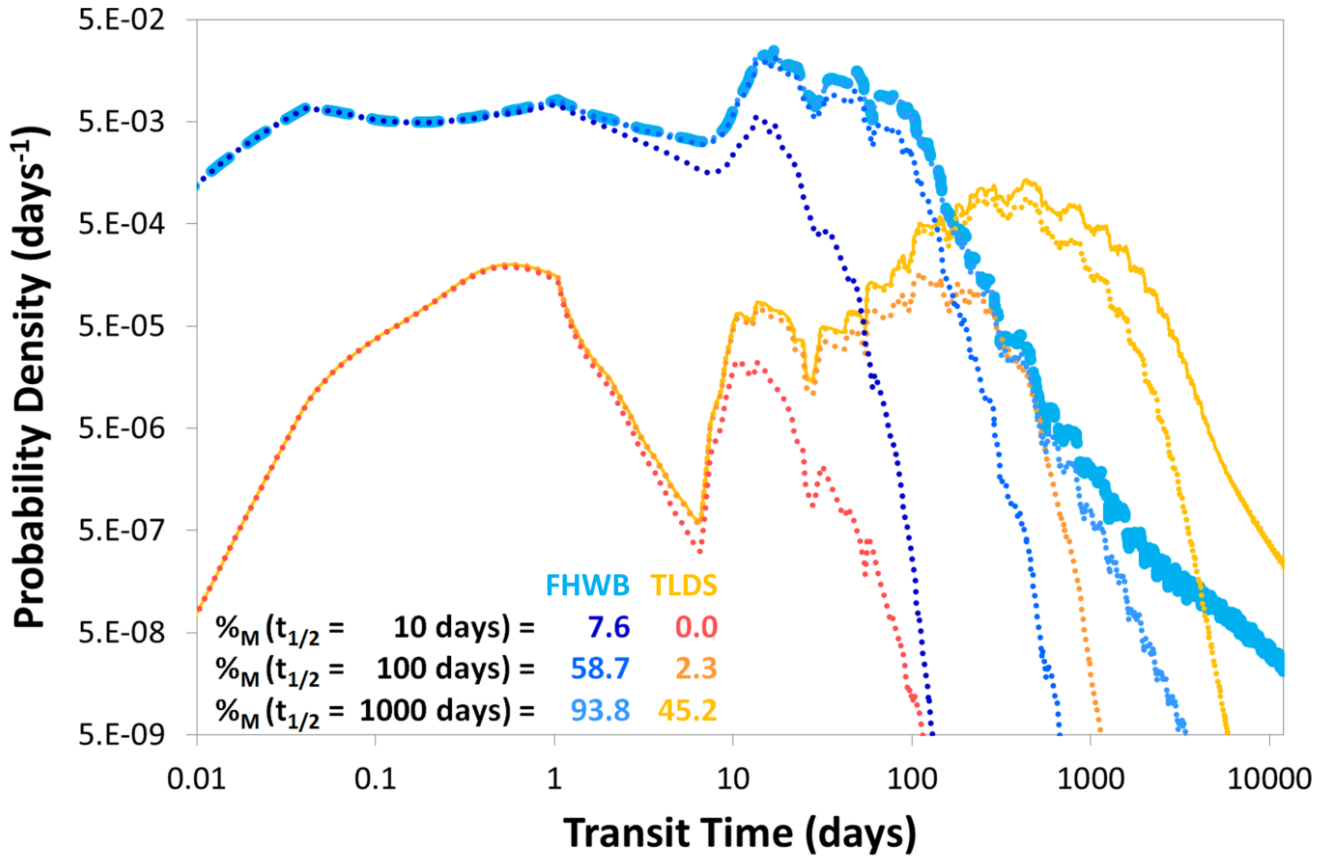
Figure S10: Two TTDs from the FHWB (blue) and TLDS (yellow) scenarios. Each one modified by three functions of exponential decay (with half-lives $t_{1/2}$ of 10, 100 and 1000 days). The fraction of mass eventually leaving the system ($\%_M$) can differ greatly: for a half-life of 100 days, the FHWB TTD still delivers 59 % of the original input to discharge while the TLDS TTD only delivers 2 %.

165

Table S1: Information on which of the base-case scenarios (upper table) the other six scenarios (porosity – blue; bedrock conductivity – orange; decay in hydraulic conductivity – red; precipitation frequency – green; soil water retention curve – purple; extreme precipitation after full saturation – yellow) are based upon.

D_{soil}							DEEP (THICK)											
K_S				HIGH									LOW				
θ_{ant}		DRY			INT			WET			DRY			INT			WET	
P_{sub}	SMALL	MED	BIG	SMALL	MED	BIG	SMALL	MED	BIG	SMALL	MED	BIG	SMALL	MED	BIG	SMALL	MED	BIG
Name	THDS	THDM	THDB	THIS	THIM	THIB	THWS	THWM	THWB	TLDS	TLDM	TLDB	TLIS	TLIM	TLIB	TLWS	TLWM	TLWB
$F_{yw\ Gam}$	0.11	0.29	0.89	0.14	0.30	0.77	0.19	0.32	0.63	0.04	0.09	0.15	0.05	0.10	0.15	0.08	0.13	0.18
$F_{yw\ Mod}$	0.01	0.03	0.11	0.05	0.11	0.26	0.18	0.25	0.40	0.00	0.01	0.08	0.01	0.03	0.12	0.05	0.12	0.20
D_{soil}							SHALLOW (FLAT)											
Name	FHDS	FHDM	FHDB	FHIS	FHIM	FHIB	FHWS	FHWM	FHWB	FLDS	FLDM	FLDB	FLIS	FLIM	FLIB	FLWS	FLWM	FLWB
$F_{yw\ Gam}$	0.27	0.84	1.00	0.28	0.74	0.96	0.30	0.60	0.86	0.09	0.17	0.23	0.11	0.17	0.24	0.14	0.19	0.25
$F_{yw\ Mod}$	0.03	0.11	0.40	0.10	0.25	0.51	0.25	0.39	0.61	0.01	0.05	0.20	0.02	0.10	0.23	0.09	0.17	0.25

Young Water Threshold: short — long
Young Water Fraction: small — large

Table S2. Young water fractions (F_{yw}) for the 36 different base-case scenarios. The young water fractions are determined from the best-fit Gamma distributions ($F_{yw\ Gam}$) and from the modeled TTDs themselves ($F_{yw\ Mod}$).

Name	THDM	1	2	3	4	5	6	7	8	9	10	11	12	13	14	15	μ	σ
1st Quartile	137	138	143	136	144	136	179	166	163	181	120	162	136	165	159	123	150	19
Median	207	220	208	245	241	227	250	251	239	246	207	244	236	242	244	204	234	16
Mean	280	277	280	286	291	280	306	300	300	302	262	296	285	298	296	265	288	13
3rd Quartile	366	357	339	358	367	360	368	363	361	366	349	362	358	355	365	351	359	8
Stand Dev	298	299	294	298	302	302	295	298	295	297	300	296	302	299	297	299	298	2.5
Skewness	14.8	15.7	15.6	15.4	15.3	15.5	15.6	15.6	15.7	15.6	15.4	15.6	15.5	15.9	15.5	15.4	15.5	0.16
Exc Kurtosis	407	433	434	423	416	422	432	432	436	433	421	433	424	439	429	422	429	6.5

short — long
wider — narrower
more skewed — less skewed
more peaked — flatter

Table S3. Distribution metrics for the 15 TTDs resulting from different precipitation event sequences. For comparison we also show the metrics for the THDM scenario which uses an actually measured time series of precipitation and has a slightly different distribution of precipitation event amounts and interarrival times but otherwise similar catchment and climate properties. The means (μ) and standard deviations (σ) of the metrics of the 15 scenarios are also shown.

References

Jasechko, S., Kirchner, J. W., Welker, J. M., and McDonnell, J. J.: Substantial proportion of global streamflow less than three months old, Nat. Geosci., 9(2), 126-129, https://doi.org/10.1038/NGEO2636, 2016.

Kellison, S. G. and London, R. L.: Risk Models and Their Estimation, Actex Publications, Winsted, USA, 2011.

Kirchner, J. W.: Aggregation in environmental systems–Part 1: Seasonal tracer cycles quantify young water fractions, but not mean transit times, in spatially heterogeneous catchments, Hydrol. Earth Syst. Sc., 20(1), 279–297, https://doi.org/10.5194/hess-20-279-2016, 2016.

Rolski, T., Schmidli, H., Schmidt, V., and Teugels, J. L.: Stochastic processes for insurance and finance, 505, John Wiley & Sons, Chichester, England, 2009.